

# Analysis by NMR Spectroscopy of the Structural Homology between the Linear and the Cyclic Peptide Recognized by Anti-human Leukocyte Antigen Class I Monoclonal Antibody TP25.99\*<sup>§</sup>

Received for publication, April 28, 2000, and in revised form, May 23, 2000  
Published, JBC Papers in Press, May 23, 2000, DOI 10.1074/jbc.M003647200

Franklin J. Moy, Smruti A. Desai<sup>‡</sup>, Xinhui Wang<sup>‡</sup>, Elvyra J. Noronha<sup>‡</sup>, Qinwei Zhou<sup>‡</sup>,  
Soldano Ferrone<sup>‡</sup>, and Robert Powers<sup>§</sup>

From the Department of Biological Chemistry, Wyeth Research, Cambridge, Massachusetts 02140  
and the <sup>‡</sup>Department of Immunology, Roswell Park Cancer Institute, Buffalo, New York 14263

The anti-human leukocyte antigen (HLA) class I monoclonal antibody (mAb) TP25.99 has a unique specificity since it recognizes both a conformational and a linear determinant expressed on the  $\beta_2\text{-}\mu$ -associated and  $\beta_2\text{-}\mu$ -free HLA class I heavy chains, respectively. Previously, we reported the identification of a cyclic and a linear peptide that inhibits mAb TP25.99 binding to the  $\beta_2\text{-}\mu$ -associated and  $\beta_2\text{-}\mu$ -free HLA class I heavy chains (S. A. Desai, X. Wang, E. J. Noronha, Q. Zhou, V. Rebmann, H. Grosse-Wilde, F. J. Moy, R. Powers, and S. Ferrone, submitted for publication). The linear X<sub>19</sub> and cyclic LX-8 peptides contain sequence homologous to residues 239–242, 245, and 246 and to residues 194–198, respectively, of HLA class I heavy chain  $\alpha_3$  domain. Analysis by two-dimensional transfer nuclear Overhauser effect spectroscopy of the induced solution structures of the linear X<sub>19</sub> and cyclic LX-8 peptides in the presence of mAb TP25.99 showed that the two peptides adopt a similar structural motif despite the lack of sequence homology. The backbone fold is suggestive of a short helical segment followed by a tight turn, reminiscent of the determinant loop region (residues 194–198) on  $\beta_2\text{-}\mu$ -associated HLA class I heavy chains. The structural similarity between the linear X<sub>19</sub> and cyclic LX-8 peptides and the lack of sequence homology suggests that mAb TP25.99 predominantly recognizes a structural motif instead of a consensus sequence.

HLA<sup>1</sup> class I antigens present peptides to cytotoxic lymphocytes and thus play a crucial role in allograft rejection and tumor surveillance. Like their counterparts in other animal species, HLA class I antigens are comprised of a polymorphic heavy chain non-covalently associated with  $\beta_2\text{-}\mu$ . The association of  $\beta_2\text{-}\mu$  to HLA class I heavy chains causes marked changes in their conformation and in their antigenic profile. This finding, with a few exceptions (2, 3), accounts for the selective reactivity of monoclonal and polyclonal allo- and xenoantibodies with either  $\beta_2\text{-}\mu$ -free or  $\beta_2\text{-}\mu$ -associated HLA class I heavy

chains. In the course of the analysis of the fine specificity of a panel of anti-HLA class I mAb, we have found that mAb TP25.99 has the unusual characteristic to react with both  $\beta_2\text{-}\mu$ -free and  $\beta_2\text{-}\mu$ -associated HLA class I heavy chains (4, 5). As described in a related paper,<sup>2</sup> this reactivity is mediated by the recognition of distinct and spatially distant antigenic determinants located in HLA class I heavy chain  $\alpha_3$  domains. One expressed on  $\beta_2\text{-}\mu$ -associated HLA class I heavy chains has been mapped to amino acid residues 194–198, and the other one expressed on  $\beta_2\text{-}\mu$ -free HLA class I heavy chains has been mapped to amino acid residues 239–242, 245, and 246. The two antigenic determinants have no homology in their amino acid sequence.

Since only the x-ray structure of  $\beta_2\text{-}\mu$ -associated HLA class I heavy chain (6, 7) has been described, the structural relationship between the two antigenic determinants in the  $\beta_2\text{-}\mu$ -free and  $\beta_2\text{-}\mu$ -associated HLA class I heavy chains is not known. To obtain this information, we have analyzed by NMR the induced solution conformation of the linear X<sub>19</sub> peptide and the cyclic LX-8 peptide in the presence of mAb TP25.99. The linear and the cyclic peptides were identified by panning a linear and a cyclic random phage display peptide library with mAb TP25.99, as described in a related paper.<sup>2</sup> Additionally, both peptides were shown to inhibit the interaction of TP25.99 with both  $\beta_2\text{-}\mu$ -free and  $\beta_2\text{-}\mu$ -associated HLA class I heavy chains with an approximate IC<sub>50</sub> of 30  $\mu\text{M}$ . The resulting solution structure of the linear X<sub>19</sub> peptide is based on a total of 133 experimental NMR distance restraints where the atomic r.m.s. distribution about the mean coordinate position for residues 4–13 is 0.87  $\pm$  0.13  $\text{\AA}$  for the backbone atoms. The resulting solution structure of the cyclic LX-8 is based on a total of 50 experimental NMR distance restraints where the atomic r.m.s. distribution about the mean coordinate position for residues 3–10 is 0.78  $\pm$  0.22  $\text{\AA}$  for the backbone atoms.

## EXPERIMENTAL PROCEDURES

**Monoclonal Antibodies**—The anti-HLA class I mAb TP25.99 (4, 5) was purified from ascitic fluid by sequential precipitation with caprylic acid and ammonium sulfate (8). The purity and activity of mAb TP25.99 preparations were assessed by SDS-polyacrylamide gel electrophoresis and enzyme-linked immunosorbent assay, respectively.

**Synthetic Peptides**—The X<sub>19</sub> (IDPVGVGNERTFFFQVPAEG) and LX-8 (QCTNFISDHECH) synthetic peptides were purchased from Syn-Pep Corp., Dublin, CA. They were synthesized using standard Fmoc (*N*-(9-fluorenyl)methoxycarbonyl) solid phase peptide synthesis in an automated peptide synthesizer (9050 Plus; Perspective Biosystems, MA). The synthetic peptide, LX-8, was cyclized using 5% dimethyl

\* The costs of publication of this article were defrayed in part by the payment of page charges. This article must therefore be hereby marked "advertisement" in accordance with 18 U.S.C. Section 1734 solely to indicate this fact.

§ The on-line version of this article (available at <http://www.jbc.org>) contains Tables I and II.

¶ To whom correspondence should be addressed: Wyeth Research, 85 Bolton St., Rm. 222B, Cambridge, MA 02140. Tel.: 617-665-7997; Fax: 617-665-8993; E-mail: powersr@war.wyeth.com.

<sup>1</sup> The abbreviations used are: HLA, human leukocyte antigen; mAb, monoclonal antibody; NOE, nuclear Overhauser effect; NOESY, nuclear Overhauser enhanced spectroscopy; r.m.s., root mean square.

<sup>2</sup> S. A. Desai, X. Wang, E. J. Noronha, Q. Zhou, V. Rebmann, H. Grosse-Wilde, F. J. Moy, R. Powers, and S. Ferrone, submitted for publication.

sulfoxide and purified by reverse phase high performance liquid chromatography. Cyclization was confirmed by mass spectroscopy. The purity of the peptides was greater than 96% as assessed by high performance liquid chromatography.

**NMR Sample Preparation**—Samples for NMR contained either 4 mM free X<sub>19</sub> or LX-8 peptide or 0.1 mM mAb TP25.99 complexed with 4 mM X<sub>19</sub> or LX-8 peptide in 90% H<sub>2</sub>O, 10% D<sub>2</sub>O or 100% D<sub>2</sub>O in a buffered solution of 100 mM potassium phosphate and 2 mM sodium azide at pH 5.5.

**NMR Data Collection**—All spectra were recorded at 25 °C on a Bruker AMX600 spectrometer using a gradient-enhanced triple resonance <sup>1</sup>H/<sup>13</sup>C/<sup>15</sup>N probe. For spectra recorded in H<sub>2</sub>O, water suppression was achieved with the WATERGATE sequence (9). Two-dimensional NOESY (10), two-dimensional TOCSY (11), and two-dimensional ROESY (12) experiments were collected. In general, the acquisition dimension was collected with a spectral width of 13.44 ppm, using 2048 real points with the carrier at 4.75 ppm. Spectral widths in the indirect detected proton dimensions were 13.44 ppm with 512 complex points. Mixing times for the NOESY, TOCSY, and ROESY experiments were 200, 49, and 200 ms, respectively. NOESY experiments collected on mAb TP25.99 complexed with the X<sub>19</sub> and LX-8 peptides used a 10-ms spin echo sequence to select for resonance from the X<sub>19</sub> or LX-8 peptide (13). The large correlation time ( $\tau_c$ ) difference between mAb TP25.99 and the peptides and the resulting increase in line widths allowed for the removal of mAb TP25.99 resonances from the spectra during the spin echo. Quadrature detection in the indirectly detected dimensions were recorded with states-time-proportional phase incrementation hypercomplex phase increment (14) and collected with appropriate refocusing delays to allow for spectra with 0,0 or -90,180 phase correction. Spectra were processed using the NMRPipe software package (15) and analyzed with PIPP (16) on a Sun Sparc Workstation.

**Interproton Distance Restraints**—The NOEs assigned from the transfer NOE experiment were classified into strong, medium, and weak corresponding to interproton distance restraints of 1.8–2.7 Å (1.8–2.9 Å for NOEs involving NH protons), 1.8–3.3 Å (1.8–3.5 Å for NOEs involving NH protons), 1.8–5.0 Å and 1.8–6.0 Å, respectively (17, 18). The upper limits for distances involving methyl protons and non-stereospecifically assigned methylene protons were corrected appropriately for center averaging (19), and an additional 0.5 Å was added to upper distance limits for NOEs involving methyl protons (20, 21).

**Structure Calculations**—Structures were calculated by the hybrid distance geometry-dynamically simulated annealing method (22) with minor modifications (23) using the program XPLOR (24), adapted to incorporate a conformational data base potential (25, 26). The target function that is minimized during restrained minimization and simulated annealing comprises only quadratic harmonic terms for covalent geometry, square-well quadratic potentials for the experimental distance and torsion angle restraints, and a quartic van der Waals term for non-bonded contacts. All peptide bonds were constrained to be planar and trans. The spectra for X<sub>19</sub> clearly indicated that the prolines in the peptide were not undergoing a cis-trans isomerization. Additionally, there was no evidence to suggest a cis-conformation for any of the prolines. There were no hydrogen bonding, electrostatic, or 6–12 Lennard-Jones empirical potential energy terms in the target function. The simulated annealing protocol followed a two-stage procedure. In the first stage, the simulated annealing structures were determined based on the experimental distance restraints similar to previous structure calculations (27–29). The resulting structures were then used as initial structures for the second stage of simulated annealing calculations where in addition to the distance restraints the structures were refined against a conformational data base potential.

## RESULTS AND DISCUSSION

**Functional and Sequence Mimicry by the Induced Conformations of the Linear X<sub>19</sub> Peptide and the Cyclic LX-8 Peptide of the Antigenic Determinants Recognized by mAb TP25.99**—Based on the amino acid sequence homology of the HLA class I heavy chain with a linear and a cyclic peptide isolated from phage display peptide libraries, the antigenic determinants recognized by mAb TP25.99 on  $\beta_2\mu$ -associated and  $\beta_2\mu$ -free HLA class I heavy chains have been previously mapped.<sup>2</sup> The conformational (LX-8) and linear (X<sub>19</sub>) determinants are expressed on residues 194–198 and residues 239–242 and 245–246, respectively, of the HLA class I heavy chain  $\alpha_3$  domain. The LX-8 and X<sub>19</sub> peptides were shown to inhibit the interaction of TP25.99 with both  $\beta_2\mu$ -free and  $\beta_2\mu$ -associated HLA

class I heavy chains with an approximate IC<sub>50</sub> of 30  $\mu$ M.<sup>2</sup> The residues from the conformational and linear determinants are identified on the x-ray structure of  $\beta_2\mu$ -associated HLA class I heavy chain (6), as shown in Fig. 1.

The HLA class I heavy chain has an overall “V”-shaped structure where  $\beta_2\mu$  fits into the corresponding cleft. The interface between  $\beta_2\mu$  and the HLA class I heavy chain  $\alpha_3$  domain is composed of two parts of the four-stranded  $\beta$ -sheets of both  $\beta_2\mu$  (strands 1 and 2) and the  $\alpha_3$  domain (strands 4 and 5), where  $\beta_2\mu$  is approximately perpendicular to the  $\alpha_3$  domain. The interface is very polar with a total of 16 hydrogen bonds, where a majority of the hydrogen bonds are between side chain and backbone atoms resulting in an intercalation of side chains between  $\beta_2\mu$  and  $\alpha_3$  domain. It is noteworthy that no information on the structure of  $\beta_2\mu$ -free HLA class I heavy chain is available. The x-ray structure does suggest that removal of  $\beta_2\mu$  would result in a significant conformational change in the HLA class I heavy chain.

It is evident from the x-ray structure of the  $\beta_2\mu$ -associated HLA class I heavy chain that residues 239–242, 245, and 246 of HLA class I heavy chains corresponding to the linear X<sub>19</sub> peptide are masked by  $\beta_2\mu$ . Therefore, the corresponding antigenic determinant becomes accessible to mAb TP25.99 only when HLA class I heavy chains are not associated with  $\beta_2\mu$ . A view of the x-ray structure of  $\beta_2\mu$ -associated HLA class I heavy chain where the  $\beta_2\mu$  subunit has been removed for clarity is shown in Fig. 1. Thus, an NMR analysis of the interaction of mAb TP25.99 with the linear X<sub>19</sub> peptide provides insight into the interaction of mAb TP25.99 with the determinant expressed on residues 239–242, 245, and 246 of  $\beta_2\mu$ -free HLA class I heavy chain  $\alpha_3$  domain. Conversely, residues 194–198 of HLA class I heavy chains that are homologous to the cyclic LX-8 peptide are freely accessible to mAb TP25.99 in the presence of  $\beta_2\mu$ . Thus these residues express the antigenic determinant recognized by mAb TP25.99 on  $\beta_2\mu$ -associated HLA class I heavy chain  $\alpha_3$  domain. Thus, an NMR analysis of the interaction of mAb TP25.99 with the cyclic LX-8 peptide provides insight into the interaction of mAb TP25.99 with the determinant expressed on residues 194–198 of  $\beta_2\mu$ -associated HLA class I heavy chain  $\alpha_3$  domain.

**NMR Resonance Assignments**—The NMR resonance assignments for the X<sub>19</sub> and LX-8 peptide are listed in supplemental Tables I and II, respectively. The assignments followed the protocol described by Wuthrich (30). NH-H $\alpha$ -expanded regions of the H<sub>2</sub>O TOCSY and NOESY spectra along with the X<sub>19</sub> peptide assignments are shown in Fig. 2. It should be noted that some side chain resonance assignments were based on expected chemical shift trends from random coil chemical shifts for the common amino acids (30). As an example, Arg<sup>10</sup> from X<sub>19</sub> exhibits side chain chemical shifts of 1.46 and 3.02 that were assigned to H $\gamma$  and H $\delta$ , respectively, based on the typical chemical shift range for these resonances.

**NMR Structure Determination of the Linear X<sub>19</sub> Peptide and the Cyclic LX-8 Peptide**—The induced structures for the X<sub>19</sub> and LX-8 peptides in the presence of mAb TP25.99 were determined from the observation of transfer NOEs in a sample containing an excess of peptide relative to mAb TP25.99 (31–33). Binding of the X<sub>19</sub> and LX-8 peptides to mAb TP25.99 is evident from the appearance of new structural NOEs and a change in the sign and intensity of NOEs in the complex relative to free peptide. In the absence of mAb TP25.99, both peptides exhibited a majority of weak positive NOEs that correlated with expected COSY peaks. For the cyclic LX-8 peptide, some NOEs attributed to the constrained nature of the peptide were observed in the free peptide that changed sign and intensity from weak positive peaks to strong negative peaks in the

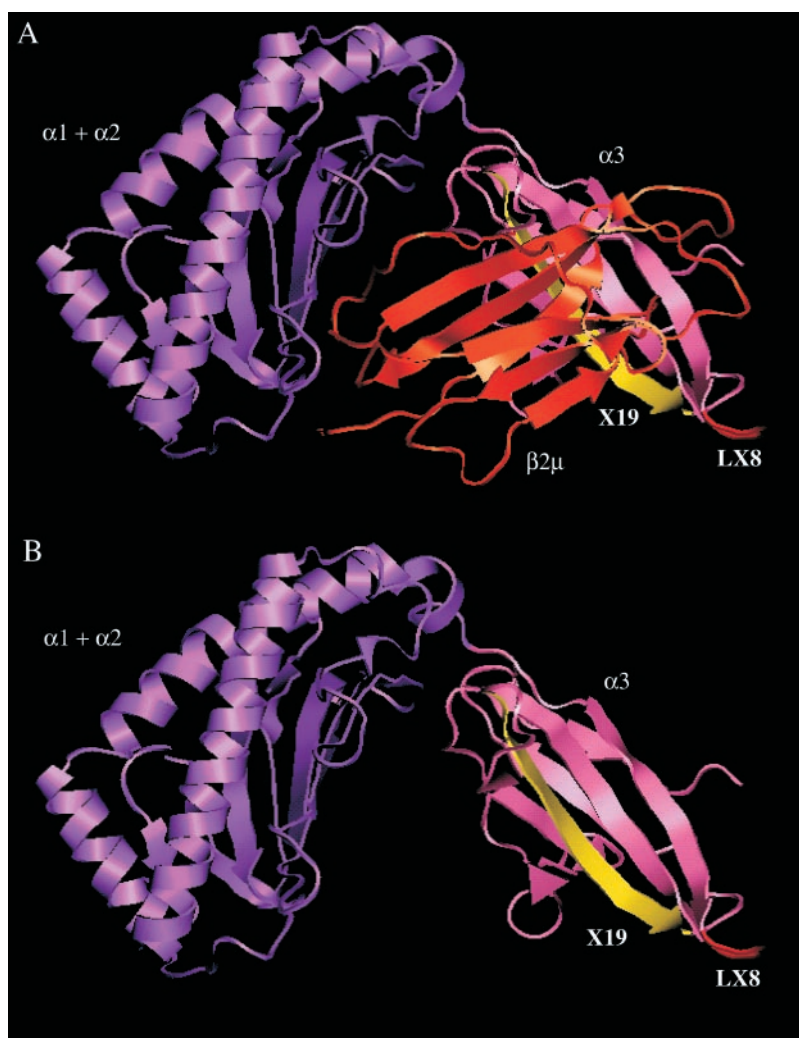


FIG. 1. Ribbon diagram of the x-ray structure of  $\beta_2$ - $\mu$ -associated (A) and  $\beta_2$ - $\mu$ -free (B) HLA class I heavy chains. The residues corresponding to the X<sub>19</sub> and to the LX-8 peptide are colored yellow and red, respectively.

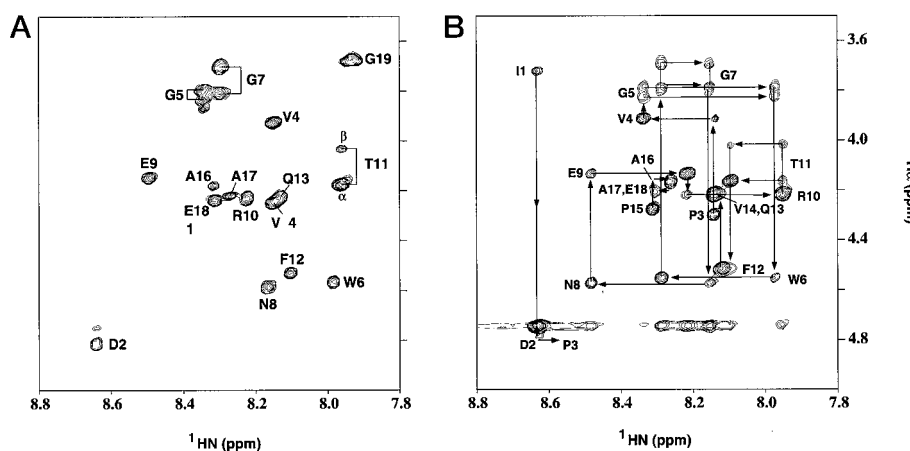


FIG. 2. Expanded NH-H $\alpha$  region of the H<sub>2</sub>O TOCSY (A) and NOESY (B) spectra for the X<sub>19</sub> peptide. Sequential assignments are indicated.

presence of mAb Tp25.99. The lack of structural NOEs for the X<sub>19</sub> and LX-8 peptides in the absence of mAb TP25.99 is consistent with a disordered conformation generally expected for small peptides. An expanded region of the NOESY spectra for the mAb TP25.99-X<sub>19</sub> peptide complex is shown in Fig. 3. The majority of the structurally important NOEs for X<sub>19</sub> occurs between a small subset of the peptide residues. They include Val<sup>4</sup>, Trp<sup>6</sup>, Asn<sup>8</sup>, Glu<sup>9</sup>, Arg<sup>10</sup>, and Phe<sup>12</sup>, which form a compact core of the X<sub>19</sub> peptide and define most of the observed structure. Residues 1-3 and 14-19 are basically ill-defined. In fact, the line widths are noticeably sharper for Ala<sup>16</sup>-Gly<sup>19</sup>, suggest-

ing a higher order of mobility. Interestingly, the NH exchange rate with D<sub>2</sub>O for the majority of the residues is slow, suggesting either hydrogen bonding or protection from the bulk water.

The major advantage in the structure determination of the cyclic LX-8 peptide is the disulfide bond between Cys<sup>2</sup> and Cys<sup>11</sup> that significantly decreases the conformational space available to the peptide. However, the disulfide bond itself is poorly defined because of a minimal number of observed restraints. A majority of the structural NOEs involved residues Asn<sup>4</sup>, Phe<sup>5</sup>, Ile<sup>6</sup>, Ser<sup>7</sup>, Glu<sup>10</sup>, and Cys<sup>11</sup> that represent the core of the peptide structure. Similar to the X<sub>19</sub> peptide, the termi-

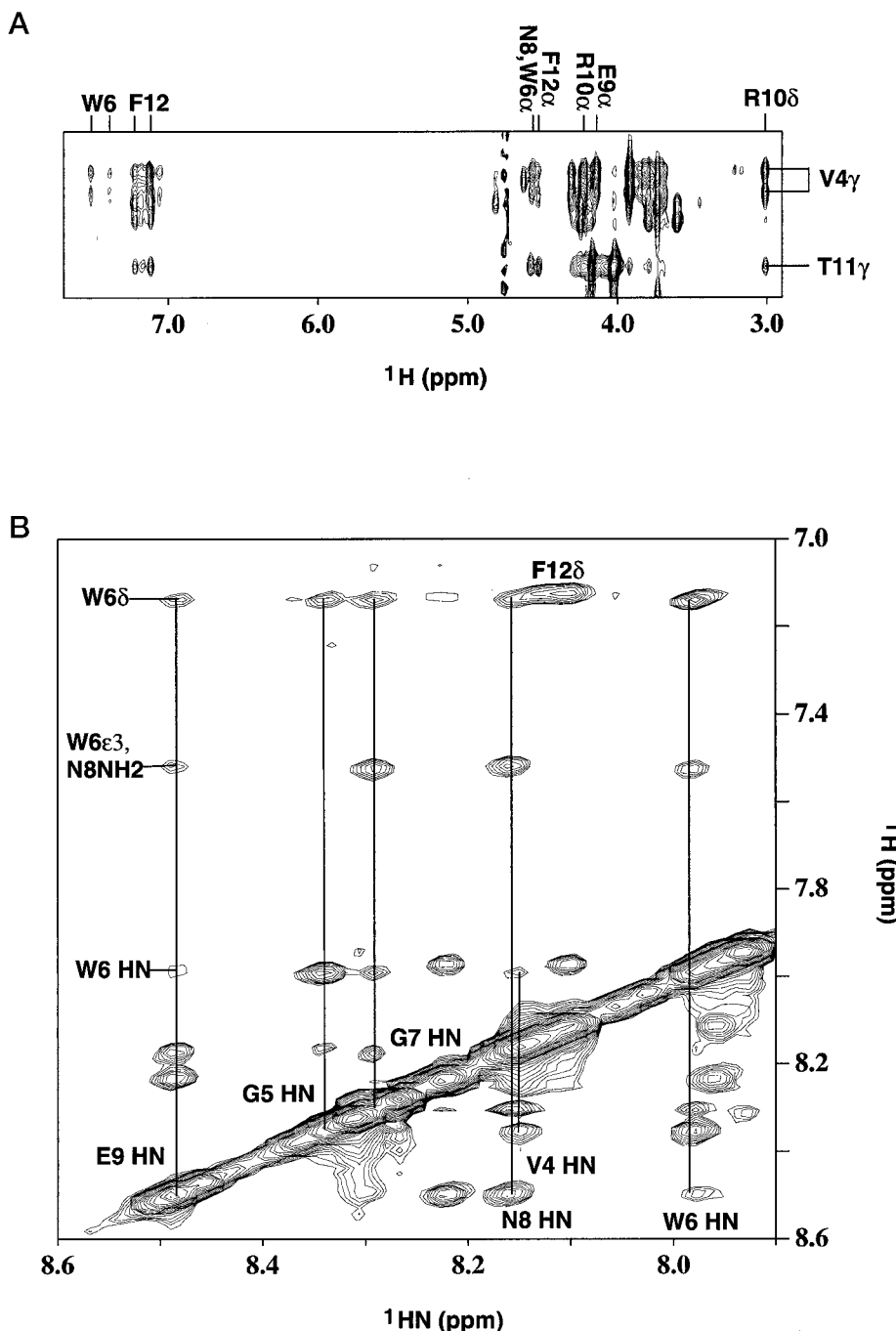


FIG. 3. Expanded region of the NOESY spectra for the mAb TP25.99-X<sub>19</sub> peptide complex. NOE assignments for the complex are indicated.

nal residues of the LX-8 peptide are poorly defined.

Proper assignments of the X<sub>19</sub> peptide NOE cross-peaks proved to be an unusually difficult task because of the following three factors: limited number of long range NOEs, a significant amount of chemical shift degeneracy, and mobility of key residues. Typically ambiguous NOE assignments can be resolved from consistency with the current refined structure that is determined from a subset of unambiguously assigned NOEs. Unfortunately, this was not the case for the X<sub>19</sub> peptide, since the number of unambiguous NOEs alone was not sufficient to define properly the structure. Therefore, proper assignments of the X<sub>19</sub> peptide NOEs resulted in a brute force method where each possible assignment was systematically explored by using ambiguous NOE definitions in XPLOR (34) until a unique set of assignments consistent with a single structure evolved. Further complications in the NOE assignments were caused by

side chain mobility. As an example, Thr<sup>11</sup> H<sub>γ</sub>2 showed unambiguous NOEs to both Asn<sup>8</sup> H<sub>α</sub> and Phe<sup>12</sup> H<sub>δ</sub>. Both NOEs are consistent with the resulting backbone structure and could be independently satisfied. However, each NOE required a different  $\chi_1$  torsion angle that could not be simultaneously satisfied. This result indicates that Thr<sup>11</sup> side chain was populating at least two distinct  $\chi_1$  angles. A similar mobility problem with the side chain of Trp<sup>6</sup> was also observed.

The NOE assignments for the LX-8 peptide were less problematic because of the disulfide bond and the cyclic nature of the peptide. The cyclic peptide structure provided a starting point to eliminate some ambiguous NOE assignments by using the inherent restriction in the structure.

The final 30 simulated annealing structures for the X<sub>19</sub> peptide were calculated on the basis of 133 experimental NMR distance restraints, 14 of which are long range ( $i - j > 4$

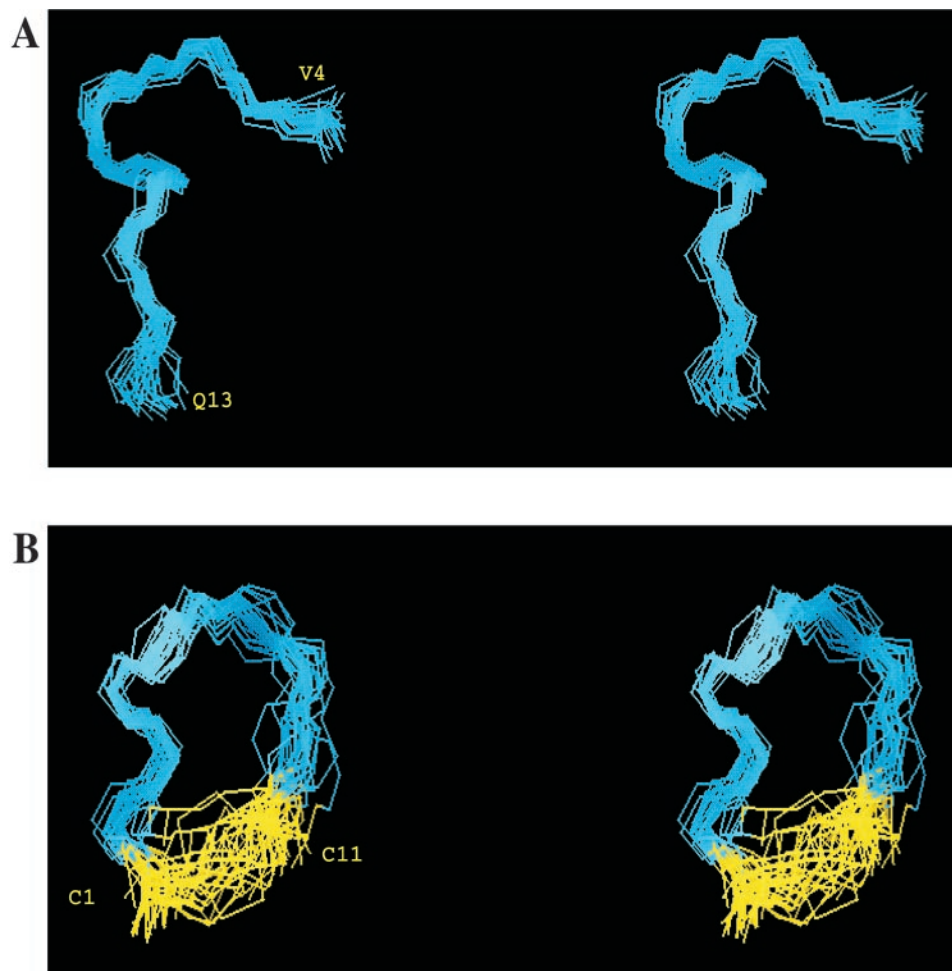


FIG. 4. Stereoview showing the best fit superposition of the backbone (nitrogen,  $\alpha$ -carbon, and carbonyl-carbon) atoms of the 30 final simulated annealing structures of the linear  $X_{19}$  peptide (A) and cyclic LX-8 peptide (B) in the presence of mAb TP25.99. Residues 4–13 are shown for  $X_{19}$ . Residues 2–11 are shown for LX-8 where the disulfide bond is colored yellow.

residues), 112 short range, and 7 intraresidues. The long range restraints were between Val<sup>4</sup> and Glu<sup>9</sup>–Phe<sup>12</sup>. The atomic r.m.s. distribution of the 30 simulated annealing structures about the mean coordinate positions for the backbone atoms of residues 4–13 is  $0.87 \pm 0.13$  Å. A best-fit superposition of the backbone atoms for residues 4–13 is shown in Fig. 4.

The final 30 simulated annealing structures for the LX-8 peptide were calculated on the basis of 50 experimental NMR distance restraints, 7 of which are long range ( $i - j = 4$  residues), 39 short range, and 4 intraresidue. The long range restraints were between Cys<sup>11</sup> and Cys<sup>2</sup> and between Asn<sup>4</sup> and Ile<sup>6</sup> and Glu<sup>10</sup>. The atomic r.m.s. distribution of the 30 simulated annealing structures about the mean coordinate positions for the backbone atoms of residues 3–10 is  $0.78 \pm 0.22$  Å. A best fit superposition of the backbone atoms for residues 3–10 is shown in Fig. 4.

**Comparison of the mAb TP25.99-induced Linear  $X_{19}$  Peptide and Cyclic LX-8 Peptide Conformations**—The solution structure for the  $X_{19}$  peptide in the presence mAb TP25.99 was determined first because of its inherent flexibility and the interest in its relationship to  $\beta_2\text{-}\mu$ -free HLA class I heavy chain. Neither the  $X_{19}$  nor the cyclic LX-8 peptide exhibited a preferred conformation in the absence of mAb TP25.99. The  $X_{19}$  peptide forms a folded backbone suggestive of a short helical section between residues Asn<sup>8</sup> and Arg<sup>10</sup> that is preceded by a sharp turn at Gly<sup>7</sup> in the presence of mAb TP25.99. Additionally, residues Val<sup>4</sup>–Trp<sup>6</sup> and Thr<sup>11</sup>–Gln<sup>13</sup> clearly exhibit a similarity to a helical twist. This finding is consistent with the  $^1\text{H}\alpha$

chemical shift index that predicts the peptide to be predominantly helical (36). It is noteworthy that dihedral restraints were not used in the simulation. Interestingly, the backbone conformation between residues Val<sup>3</sup>–Asn<sup>8</sup> also suggests a similarity to a small cyclic peptide, a common approach for mimicking protein turn regions. As stated previously, the NH exchange rate with D<sub>2</sub>O for the majority of the residues is slow. This observation is consistent with the proposed structure for the  $X_{19}$  peptide where sequential hydrogen bonds in the helical and loop region would be expected. Additionally, the slow NH exchange rates may result from the amides being shielded from the bulk solvent by the interaction of the peptide with mAb TP25.99. It is probable that the observed slow NH exchange rates are a result of both factors providing further support for the accuracy of the bound conformation of the  $X_{19}$  peptide. Hydrogen bond constraints were not used in the refinement of the  $X_{19}$  peptide structure.

The partial similarity of the  $X_{19}$  peptide to a cyclic peptide became even more apparent upon the completion of the LX-8 NMR solution structure in the presence of mAb TP25.99. It was rather obvious that a similar structural motif was present in the LX-8 peptide, a sharp turn followed by a short helical region. An unusual characteristic of the alignment of  $X_{19}$  with LX-8 is the directionality of the peptide backbones. The observed backbone conformation for the LX-8 peptide runs in the opposite direction relative to the  $X_{19}$  peptide. An alignment of the backbone atoms for residues 4–11 for the  $X_{19}$  peptide with residues 10–3 for the LX-8 peptide yielded an atomic r.m.s. of

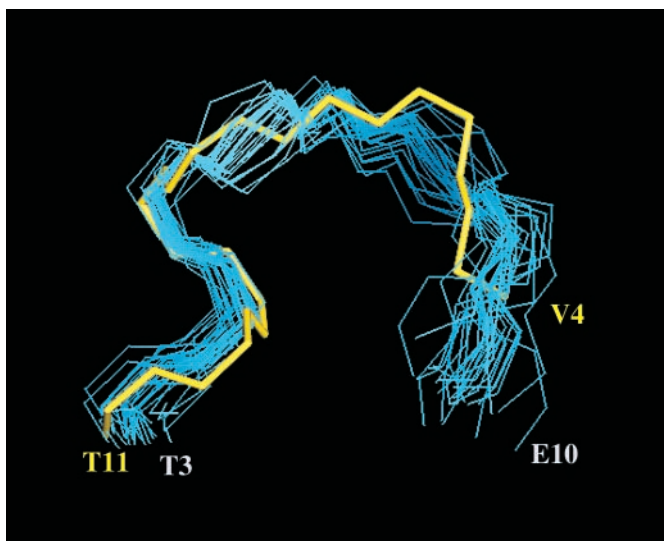


FIG. 5. The best fit superposition of the backbone (nitrogen,  $\alpha$ -carbon, and carbonyl-carbon) atoms of the restrained minimized average structure for LX-8 (yellow) and the 30 final simulated annealing structures of the  $X_{19}$  peptide (blue).

1.06 Å. A superposition of the backbone atoms of the average restrained-minimized structure of the LX-8 peptide and the ensemble of the final 30 structures for the  $X_{19}$  peptide are shown in Fig. 5. This figure clearly demonstrates the close similarity in the overall conformation of these two peptides in the presence of mAb TP25.99. A comparison between an ensemble and an average structure conveys the relative resolution of the two structures while indicating that the average structure from one peptide falls within the ensemble of structures for the other peptide. There is little information from this structural alignment to suggest any consensus sequence that mAb TP25.99 might recognize since there is a complete lack of sequence homology between these two peptides. Additionally, because of the minimal number of NOEs and the observed mobility, the side chain orientations are not highly defined.

**Homology of the mAb TP25.99-induced Linear  $X_{19}$  Peptide and Cyclic LX-8 Peptide Conformations with the HLA-A2 Antigen X-ray Structure**—The  $\beta_2\text{-}\mu$ -associated HLA class I heavy chain  $\alpha_3$  domain consists of two  $\beta$ -sheets composed of four and three  $\beta$ -strands, respectively, and six loops (6, 7). The sequence of the cyclic LX-8 peptide is homologous to the conformational determinant sequence corresponding to a surface-exposed loop between  $\beta$ -strands 1 and 2 in the x-ray structure of the HLA class I heavy chain  $\alpha_3$  domain. In contrast, the sequence of the linear  $X_{19}$  peptide is homologous to the linear determinant sequence corresponding to part of  $\beta$ -strand 5 that forms a binding interface with  $\beta_2\text{-}\mu$ . Analysis of the probability of randomly matching a peptide with either the conformational determinant or the linear determinant based on the sequence homology observed with the cyclic LX-8 and linear  $X_{19}$  peptide was determined to be a very rare event (probability  $<0.00155$  for  $X_{19}$  and  $<0.000048$  for LX-8). Based on the observed sequence homology and the probability analysis, a correlation between the interaction of mAb TP25.99 and the peptides with the interaction of mAb TP25.99 and the intact HLA class I heavy chains  $\alpha_3$  domain is implied. Therefore, neither a homologous amino acid sequence nor a structural similarity was identified between the distinct determinants recognized by mAb TP25.99 on HLA class I heavy chains  $\alpha_3$  domain. Furthermore, there is no structural similarity between the NMR structure (Figs. 4 and 5) of the  $X_{19}$  peptide and the corresponding linear determinant in the x-ray structure of  $\beta_2\text{-}\mu$ -associated HLA class I heavy chains (Fig. 1). The cyclic LX-8 peptide has

no sequence similarity to the  $X_{19}$  peptide and corresponds to a surface-exposed loop in the x-ray structure of  $\beta_2\text{-}\mu$ -associated HLA class I heavy chains. There is an obvious structural similarity between the cyclic LX-8 peptide and the surface-exposed loop in the x-ray structure of  $\beta_2\text{-}\mu$ -associated HLA class I heavy chains suggesting that mAb TP25.99 is recognizing a common structural feature. The loop region exhibits low B-factors in the x-ray structure suggesting that the loop is not conformationally flexible where the loop is equally accessible in both the  $\beta_2\text{-}\mu$ -associated and  $\beta_2\text{-}\mu$ -free HLA class I heavy chains. Upon linearization of LX-8, the cyclic peptide loses its reactivity with mAb TP25.99.<sup>2</sup> These results taken in composite with the NMR structures of the  $X_{19}$  and LX-8 peptides suggest that mAb TP25.99 does not recognize a specific amino acid sequence but recognizes a specific structural motif. Analysis of the overlay of the backbone atoms of the  $X_{19}$  peptides for residues Val<sup>4</sup> to Arg<sup>10</sup> in Fig. 5 indicates a conformation similar to that of the cyclic peptide LX-8 or more importantly a loop region consistent with the determinant site defined by mAb TP25.99. These findings may also explain the requirement for the additional four amino acids at the C terminus in the  $X_{19}$  peptide for the expression of the determinant defined by mAb TP25.99. These residues do not play a direct role in the folding topology of the peptide or in its interaction with mAb TP25.99. Their presence in the sequence may, however, allow for the peptide structure to occur by providing extra length to the peptide without inducing or stabilizing other viable conformations (1, 35).

As discussed in detail in our related article,<sup>2</sup> the  $X_{19}$  peptide represents a determinant site recognized by mAb TP25.99 on  $\beta_2\text{-}\mu$ -free HLA class I heavy chain  $\alpha_3$  domains. Currently, no information is available about the conformation of  $\beta_2\text{-}\mu$ -free HLA class I heavy chain  $\alpha_3$  domain. The association of  $\beta_2\text{-}\mu$  to HLA class I heavy chain  $\alpha_3$  domains causes a marked change in their antigenic profile and in their conformation. Therefore, the NMR structure of the  $X_{19}$  peptide may suggest that residues corresponding to the linear determinant in the HLA class I heavy chain  $\alpha_3$  domain are capable of readily adopting the observed NMR conformation of the  $X_{19}$  peptide in the presence of mAb TP25.99. In addition, the observed NMR structure of the  $X_{19}$  peptide may imply the local conformational change that occurs upon dissociation of  $\beta_2\text{-}\mu$  from HLA class I heavy chain.

**Conclusion**—The induced solution conformation of the 19-residue linear  $X_{19}$  peptide and of the 12-residue cyclic LX-8 peptide in the presence of mAb TP25.99 is presented. The peptides that were identified by their ability to inhibit the binding of mAb TP25.99 to HLA class I antigens are composed of a backbone fold reminiscent of a sharp turn with a short helical region with opposite directionality. The sequence homology between the linear  $X_{19}$  peptide and residues 239–242, 245, and 246 of the HLA class I heavy chain  $\alpha_3$  domain identifies the determinant site recognized by mAb TP25.99 on  $\beta_2\text{-}\mu$ -free HLA class I heavy chains to this region of the  $\alpha_3$  domain. Probability analysis indicates that this event is an unlikely random occurrence. Furthermore, the described NMR conformation of the  $X_{19}$  peptide suggests a possible conformation of the  $\alpha_3$  domain in  $\beta_2\text{-}\mu$ -free HLA class I heavy chains. The lack of sequence homology between the linear  $X_{19}$  peptide and the cyclic LX-8 peptide and the corresponding regions of HLA class I heavy chain  $\alpha_3$  domain reacting with mAb TP25.99 is consistent with the possibility that this mAb recognizes primarily a structural motif as opposed to a consensus sequence. This conclusion is supported by the similarity of the backbone structure of the  $X_{19}$  peptide with the conformation of the loop region of  $\beta_2\text{-}\mu$ -associated HLA class I heavy chains and with the NMR conformation of the cyclic LX-8 peptide expressing the conformational antigenic determinant recognized by mAb TP25.99.

**Acknowledgment**—We thank Roger French for the probability analysis of the sequence match between the peptides and HLA class I heavy chain  $\alpha_3$  domain.

## REFERENCES

1. Tsou, C.-L. (1988) *Biochemistry* **27**, 1809–1812
2. Quaranta, V., Walker, L. E., Ruberto, G., Pellegrino, M. A., and Ferrone, S. (1981) *Immunogenetics* **13**, 285–295
3. Bushkin, Y., Posnett, D. N., Pernis, B., and Wang, C. Y. (1986) *J. Exp. Med.* **164**, 458–473
4. D'Urso, C. M., Wang, Z., Cao, Y., Tatsuke, R., Zeff, R. A., and Ferrone, S. (1991) *J. Clin. Invest.* **87**, 284–292
5. Tanabe, M., Sekimata, M., Ferrone, S., and Takiguchi, M. (1992) *J. Immunol.* **148**, 3202–3209
6. Madden, D. R., Garboczi, D. N., and Wiley, D. C. (1993) *Cell* **75**, 693–708
7. Saper, M. A., Bjorkman, P. J., and Wiley, D. C. (1991) *J. Mol. Biol.* **219**, 277–319
8. Temponi, M., Kageshitea, T., Perosa, F., Ono, R., Okada, H., and Ferrone, S. (1989) *Hybridoma* **8**, 85–95
9. Piotto, M., Saudek, V., and Sklenar, V. (1992) *J. Biomol. NMR* **2**, 661–665
10. Jeener, J., Meier, B. H., Bachmann, and Ernst, R. R. (1979) *J. Chem. Phys.* **71**, 4546–4553
11. Bax, A., and Davis, D. G. (1985) *J. Magn. Reson.* **65**, 355–360
12. Bothner-By, A. A., and Shukla, R. (1988) *J. Magn. Reson.* **77**, 524–535
13. Glaudemans, C. P. J., Lerner, L., Daves, G. D., Jr., Kovac, P., Venable, R., and Bax, A. (1990) *Biochemistry* **29**, 10906–10911
14. Marion, D., Ikura, M., Tschudin, R., and Bax, A. (1989) *J. Magn. Reson.* **85**, 393–399
15. Delaglio, F., Grzesiek, S., Vuister, G. W., Zhu, G., Pfeifer, J., and Bax, A. (1995) *J. Biomol. NMR* **6**, 277–293
16. Garrett, D. S., Powers, R., Gronenborn, A. M., and Clore, G. M. (1991) *J. Magn. Reson.* **95**, 214–220
17. Clore, G. M., Nilges, M., Sukumaran, D. K., Bruenger, A. T., Karplus, M., and Gronenborn, A. M. (1986) *EMBO J.* **5**, 2729–2735
18. Williamson, M. P., Havel, T. F., and Wuethrich, K. (1985) *J. Mol. Biol.* **182**, 295–315
19. Wuethrich, K., Billeter, M., and Braun, W. (1983) *J. Mol. Biol.* **169**, 949–961
20. Clore, G. M., Gronenborn, A. M., Nilges, M., and Ryan, C. A. (1987) *Biochemistry* **26**, 8012–8023
21. Wagner, G., Braun, W., Havel, T. F., Schaumann, T., Go, N., and Wuethrich, K. (1987) *J. Mol. Biol.* **196**, 611–639
22. Nilges, M., Clore, G. M., and Gronenborn, A. M. (1988) *FEBS Lett.* **229**, 317–324
23. Clore, G. M., Appella, E., Yamada, M., Matsushima, K., and Gronenborn, A. M. (1990) *Biochemistry* **29**, 1689–1696
24. Brunger, A. T. (1993) *X-PLOR*, Version 3.1 Manual, Yale University, New Haven, CT
25. Kuszewski, J., Gronenborn, A. M., and Clore, G. M. (1996) *Protein Sci.* **5**, 1067–1080
26. Kuszewski, J., Gronenborn, A. M., and Clore, G. M. (1997) *J. Magn. Reson.* **125**, 171–177
27. Clore, G. M., and Gronenborn, A. M. (1991) *Science* **252**, 1390–1399
28. Moy, F. J., Seddon, A. P., Boehlen, P., and Powers, R. (1996) *Biochemistry* **35**, 13552–13561
29. Powers, R., Garrett, D. S., March, C. J., Frieden, E. A., Gronenborn, A. M., and Clore, G. M. (1993) *Biochemistry* **32**, 6744–6762
30. Wuethrich, K. (1986) *NMR of Proteins and Nucleic Acids*, John Wiley & Sons, Inc., New York
31. Clore, G. M., and Gronenborn, A. M. (1982) *J. Magn. Reson.* **48**, 402–417
32. Clore, G. M., and Gronenborn, A. M. (1983) *J. Magn. Reson.* **53**, 423–442
33. Ni, F. (1994) *Prog. Nucl. Magn. Reson. Spectrosc.* **26**, 517–606
34. Nilges, M. (1995) *J. Mol. Biol.* **245**, 645–660
35. Jing, G.-Z., Zhou, B., Xie, L., Liu, L.-J., and Liu, Z.-G. (1995) *Biochim. Biophys. Acta* **1250**, 189–196
36. Wishart, D. S., Sykes, B. D., and Richards, F. M. (1992) *Biochemistry* **31**, 1647–1651